EGTRIB Journal
JOURNAL OF
THE EGYPTIAN SOCIETY OF TRIBOLOGY
VOLUME 20, No. 4, October 2023, pp. 106 - 116 **ISSN 2090 - 5882**
(Received June 09. 2023, Accepted in final form September 08. 2023) **jest.journals.ekb.eg**

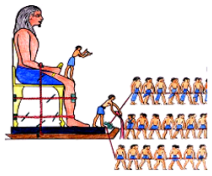

WIND SPEED SENSOR BASED ON SLIDING TRIBOELECTRIC NANOGENERATOR

Rashed A., Al-Kabbany A. M., Zeinab A. H., Youness K. A., Ali W. Y. and Ameer A. K.

Department of Production Engineering and Mechanical Design, Faculty of Engineering, Minia University, El-Minia, EGYPT.

ABSTRACT

As we progress further and further into the 21st century, the need for more sustainable sensors in the new internet of things (IoT) era has become clear. In this paper, a cheap and effective self-powered sensor was made using commercial polyamide (PA) and polytetrafluoroethylene (PTFE). The sensor is based on the sliding mode triboelectric nanogenerator (TENG) and it consists of a rotating dielectric made of PTFE and stationary dielectric-electrode pairs made from PA and aluminum.

The sensor was found to be effective as a self-powered one, outputting a maximum voltage of 2.6 V at a 100 MΩ resistive load and a current of 0.0625 ηA at a 10 MΩ resistive load. The maximum power output was 0.145 ηW at a resistive load of 40 MΩ. Although the power output was low, the high voltage output confirmed its usability as a self-powered sensor. The TENG-based sensor was then calibrated and was found to have a voltage sensitivity of 0.3626 V / (ms^{-1}) and a rotational speed sensitivity of 0.3083 rps / (ms^{-1}). Having two wind-speed-dependent variables increase the reliability of the sensor. This sensor is promising as cheap alternative to the already present self-powered wind speed sensors.

KEYWORDS

Triboelectric nanogenerator, polytetrafluoroethylene, polyamide, wind speed, self-powered sensor.

INTRODUCTION

Due to the enormous number of electronic devices, their wide distribution, and difficulties in tracking and recycling them in order to reduce their negative environmental impact, it will become impractical and possibly health hazardous for sensor networks to run only on batteries. Therefore, self-powered sensors are desperately needed for independent and continuous operations.

The phenomenon known as triboelectrification occurs when two surfaces come into contact and an electrostatic charge (ESC) is produced on both surfaces, [1 - 4]. The generated ESC by sliding or contact-separation, can be harmful, [5]. Transverse sliding generally generates higher ESC than contact and separation, [6].
To know the sign and intensity of the generated ESC from triboelectrification, the triboelectric series was developed. Assuming all other factors remain constant, the higher the potential difference between two materials in the triboelectric series the further apart they are from one another. The top of the triboelectric series has positive materials (easy to lose electrons), while the bottom of the series has negative materials (easy to gain electrons), [7 - 9].

In order to use the ESC generated from triboelectrification, the triboelectric nanogenerator (TENG) was made. It uses a combination of contact triboelectrification and electrostatic induction in order to generate power, [10]. It has been greatly successful as both an energy harvester, [11 - 15] and has been used in making many self-powered sensors, [16 - 20].

One of the possible designs of a TENG is the sliding TENG. it is structurally composed of two plates. The two plates are kept in parallel to each other and the triboelectric surfaces are in intimate contact. As they are driven by a mechanical motion/vibration acting parallel to the two plates, the two plates slide against each other while power is generated through electrostatic induction, [21 - 23].

Wind energy systems are gaining popularity as an important aspect of future renewable energy systems. For this reason, researchers have studied self-powered wind speed sensors extensively. One of which works as a sustainable power source as well as a self-powered wind speed sensor. It uses the rolling motion of PTFE beads, which serve as freestanding layers. Under a wind speed of 20 m/s, the TENG delivered a voltage of up to 17.8 V, an output current of 5.3 μA, and an output power density of 1.36 mW/cm^2, [24]. A self-powered wind sensor system that was inspired by an anemometer TENG (which is of the freestanding type) and a wind vane TENG (of the single-electrode TENG type) is proposed for measuring wind speed and direction. The anemometer TENG could output an open-circuit voltage of 88 V and short-circuit current of 6.3 μA, and a maximum power output of 0.47 mW (wind speed of 6.0 m/s), [25].

In the present work, a TENG that harvests mechanical energy driven by wind that works as a self-powered wind speed sensor is made and tested. The two surfaces of the TENG were made of polytetrafluoroethylene (PTFE) and polyamide (PA) due to their location in the triboelectric series, [6, 7].

EXPERIMENTAL

The sensor was made from a wooden structure with two wooden disks separated by four wooden bars. A through hole was drilled in the upper disc and a blind hole was drilled in the lower disc to allow the metal rod to be inserted through the top disk and stop at the end of the blind hole in the bottom disk. To allow the rod to rotate with

less resistance, two plastic buttons with holes close in diameter to the rod were placed with one of their holes in line with the holes on the top disk and the bottom disk to provide less friction. The metal rod rotated by wind using four foam plates connected to rods that all met and were adhered to the rotating rod at the center. The placement of the plates allowed the TENG to rotate when the wind blew at the foam plates. A picture of the device is shown in Fig. 1.

Attached to every wooden bar was a dielectric-electrode pair positioned at a 30° angle compared to the radius of the wooden discs. A rotating part (could be a dielectric or a dielectric-electrode pair) was also attached to the rotating metal rod so it would contact and slide along the stationary dielectric electrode pair. The dimensions of each part of the TENG are shown in Fig. 2

Different pairs of materials were tested to arrive at the best choice of materials for the TENG that can provide the highest voltage. First, a piece of PTFE (dielectric material) made from 0.1 mm thick PTFE tape was adhered to a piece of 0.05 mm thick aluminum (Al) foil, that represents a rotating dielectric-electrode pair. Four glass planes were then adhered to an Al electrode, that were used as stationary positive dielectric-electrode pairs. The voltage output of this device was measured using a Uni-T UT33A+ digital multimeter. the voltage output for this setup peaked at less than 0.001 volts between one of the stationary electrodes and the rotating electrode.

Then, the negative electrode was replaced with a polycarbonate (PC) dielectric placed on the PTFE surface, while keeping the same positive Al electrodes and glass dielectrics. The voltage output for this setup was measured, and it was found to peak at 0.06 volts between one of the stationary electrodes and a reference electrode.

The glass planes were then replaced with Polyamide (PA) meshes, made from strands that are 0.75 mm, on the positive electrodes while having a rotating negative Al electrode with a PTFE dielectric contacting the PA stationary dielectrics. The voltage output of this setup was measured and found to peak at 0.03 volts between one of the stationary electrodes and the rotating electrode.

To make the final TENG design, the previously mentioned PC-PTFE rotating part was used, with PTFE contacting and sliding along the stationary dielectric-electrode pairs which were made from the PA meshes as dielectrics placed on Al electrodes. The voltage of this setup was measured between one of the Al electrodes and a reference electrode and was found to be around 0.13 volts. Which was the highest voltage value.

Measuring voltage using an Arduino Uno was deemed more accurate than a multimeter because it can measure at a higher rate than a multimeter. A code was written and uploaded to an Arduino Uno to measure the potential difference between one of the conducting positive electrodes and the reference electrode in different conditions, the measuring circuit is shown in Figs. 3 and 4.

In order to characterize the output (voltage and current) of the TENG under different resistances, the voltage output of the TENG was measured while connecting the TENG with different resistances ranging from 1 MΩ to 200 MΩ. Then, to use the Arduino as an ammeter, the potential difference was measured across only one 10 MΩ resistor, and then the potential difference across that resistance was divided by the value of the resistance to get the current. The TENG would run for 20 seconds while the voltage and current outputs of the TENG were being measured for each resistance tested. The average of the voltage and current peaks during the test run resulting from the PTFE rotating part touching the PA dielectric whose electrode is connected to the circuit (dielectric-electrode pair colored red in Fig. 4).

To calibrate the sensor, the TENG was tested at a constant resistance and the voltage output of the TENG was measured under different wind speeds. Wind speeds were measured by a Uni-T UT363 mini anemometer. Different wind speeds were provided by a fan, the wind speed values were 2.5 m/s, 3 m/s, 3.5 m/s, 4 m/s, 4.5 m/s, 5 m/s, and 5.5 m/s.

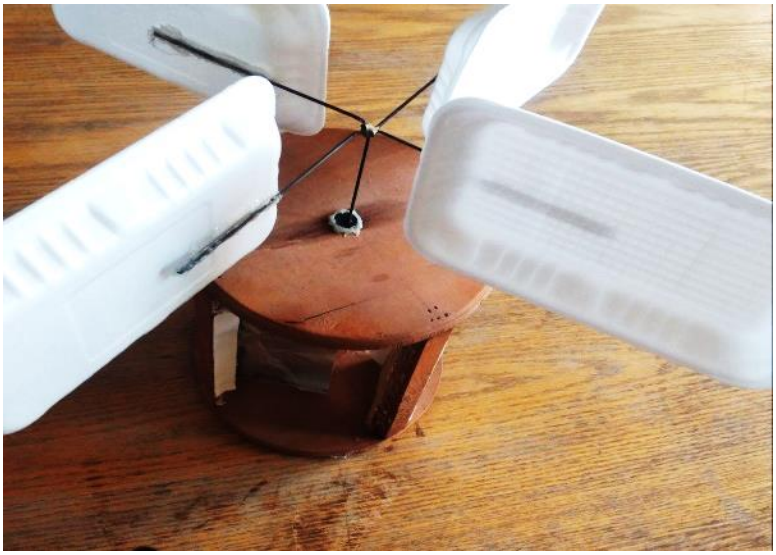

Fig. 1 The tested TENG.

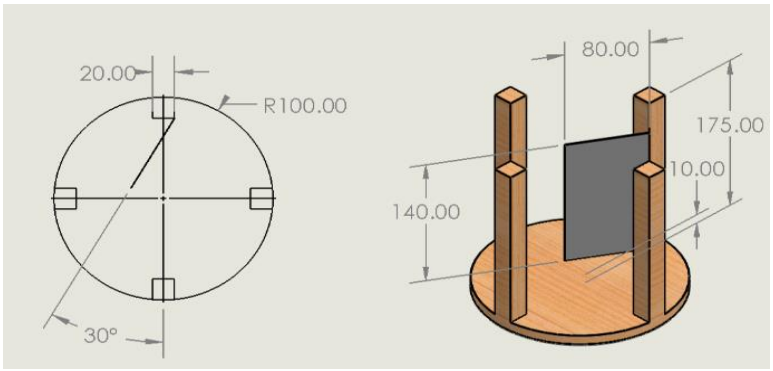

Fig. 2 Dimensions of the TENG.

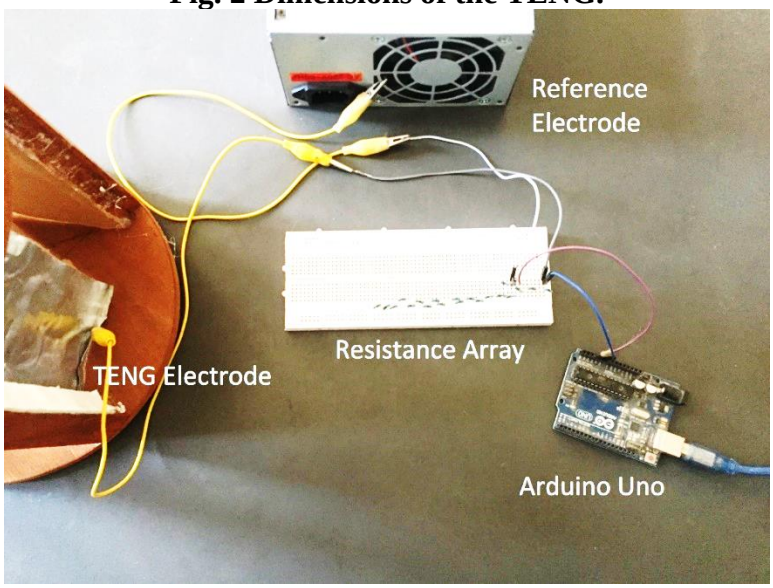

Fig. 3 Picture of the measurement setup.

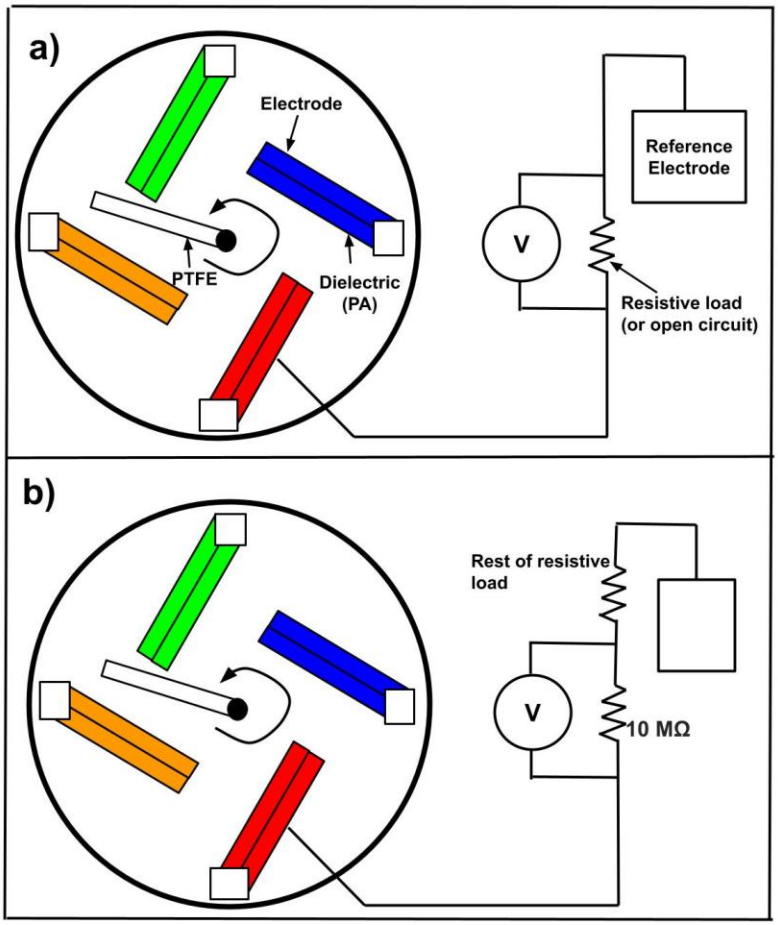

Fig. 4 (a) Voltage measuring circuit, (b) Current measuring circuit.

RESULTS AND DISCUSSION

First, the TENG was rotated by hand at open circuit condition while voltage was measured between only one TENG electrode and a reference electrode. It was found that signals of varying sign and strength were detected when the rotating dielectric contacted and slid across every stationary dielectric as shown in Fig. 5. It was illustrated that the TENG sensor can measure partial rotation as well under open circuit conditions. In order to explain the signals generated when the rotating dielectric contacts other dielectrics apart from the one whose electrode is connected to the circuit, the dielectric-electrode pair colored orange in Fig. 4a was replaced with a 2.5 mm thick polymethylmethacrylate (PMMA) dielectric layer with no electrode, the signal still persisted. This indicates that this signal is produced by the presence of the dielectric layer in the original pair, not the electrode.

The proposed explanation for this phenomenon is thus provided in Fig. 6. As the rotating dielectric contacts the dielectric layer whose electrode is connected to the circuit (red electrode), it outputs a negative signal as expected due to the negatively charged PTFE attracting positive charges from the reference electrode to the red electrode. The signals generated when the rotating dielectric contacts the orange pair's dielectric layer can be explained by a sudden decrease in the electric field between the red dielectric and the PTFE rotating dielectric due to an increase in the material separating both surfaces. This increases the dielectric constant of the space separating the red dielectric-electrode pair and the PTFE surface. This can also explain the positive sign of said signal as the decrease in the electric field between the PTFE dielectric and the red dielectric-electrode pair causes negative electrons to flow to the red dielectric.

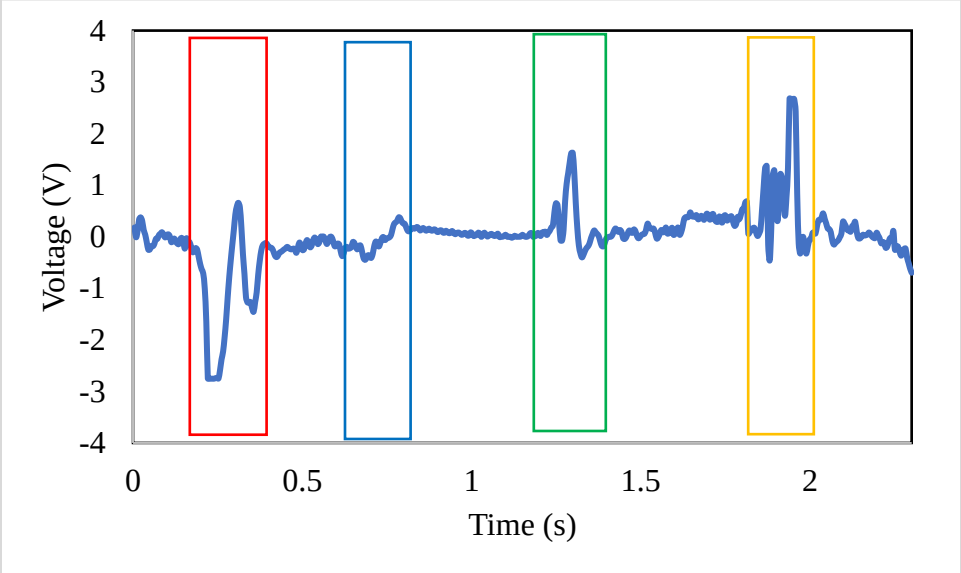

Fig. 5 Voltage response of the TENG during a full rotation under open-circuit conditions. Every colored region corresponds to the signal generated when the

rotating dielectric slid across every stationary dielectric. The colors of the regions correspond to the colors of the dielectrics shown in Fig. 4.

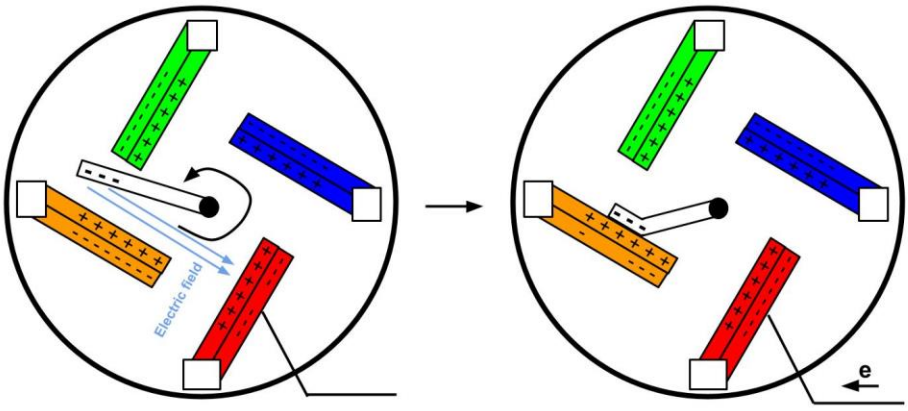

Fig. 6 Signal generation through suppression of electric field.

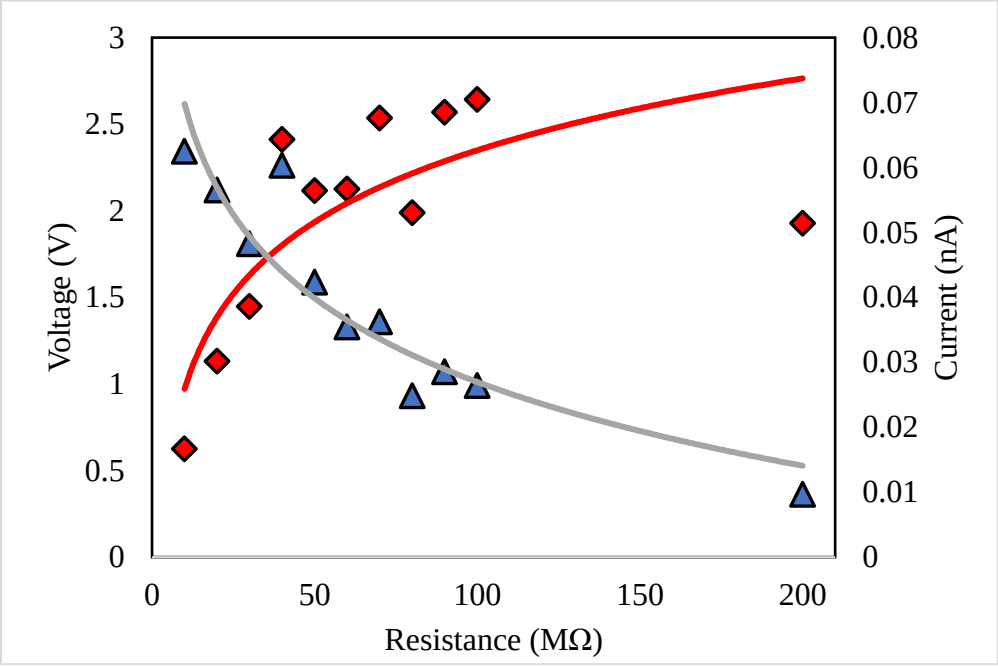

Fig. 7 Voltage and current values under different resistances under 4 m/s wind speed (with logarithmic trendlines).

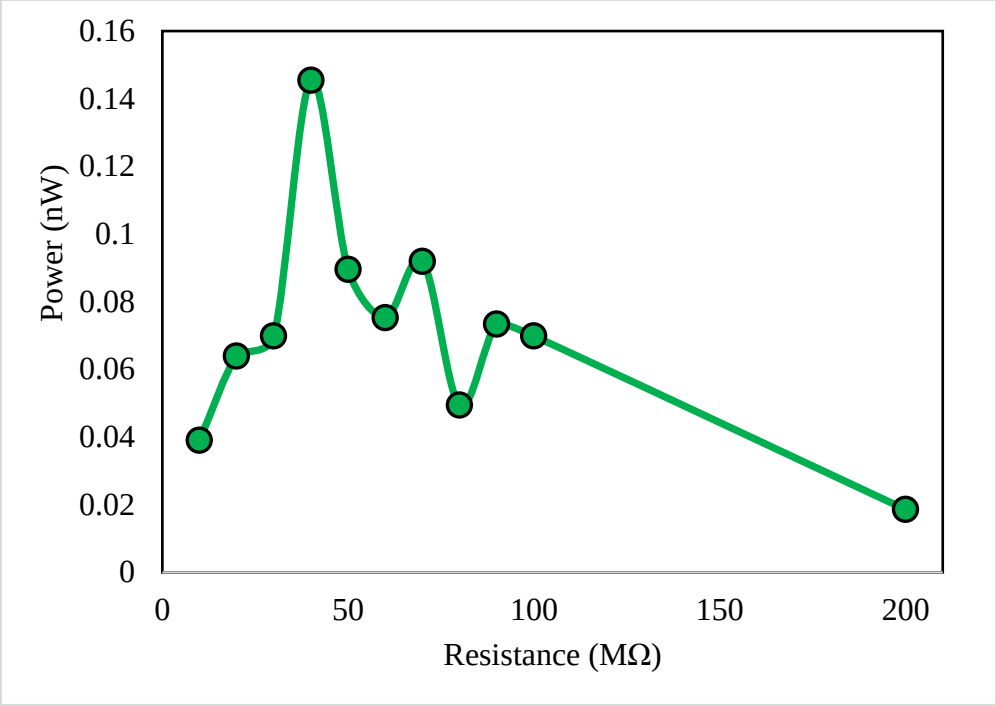

Fig. 8 Power output of the TENG under various resistances (4 m/s wind speed).

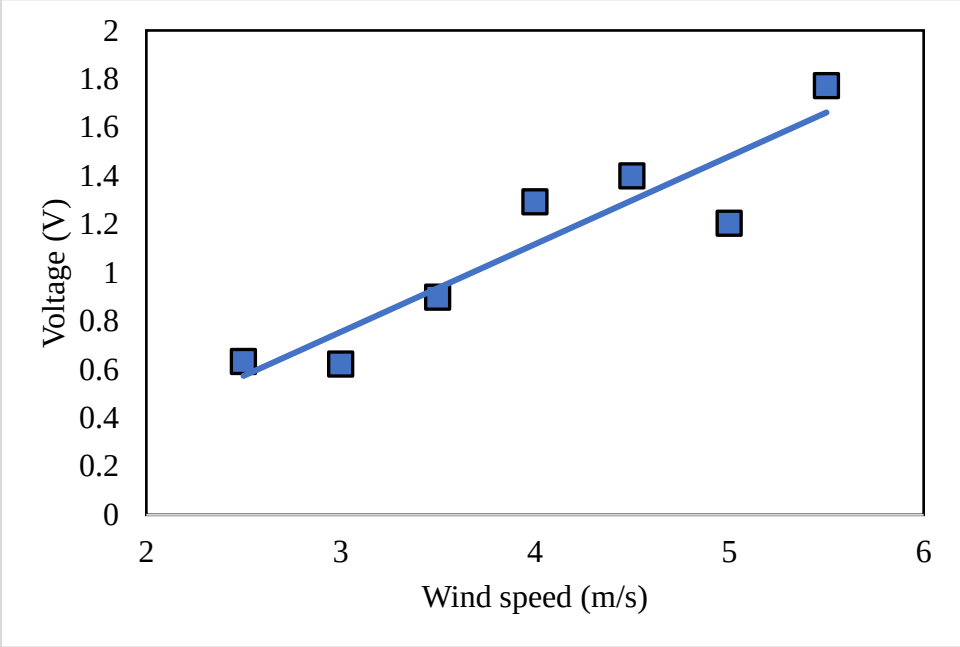

Fig. 9 Relationship between TENG voltage and wind speed under a 40MΩ resistance.

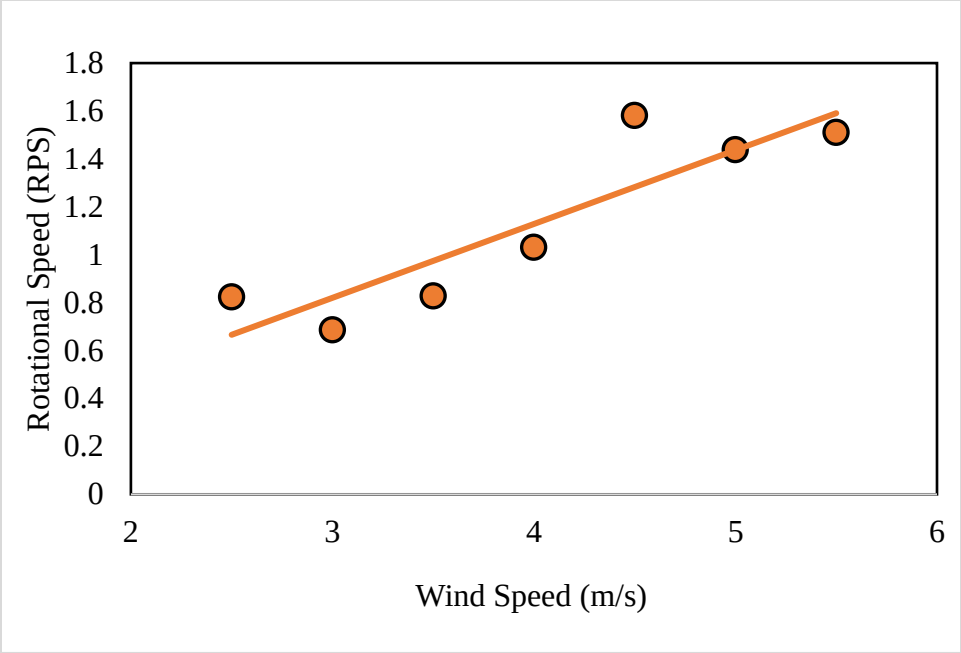

Fig. 10 Relationship between TENG rotational speed in rotations per second (rps) and wind speed.

The optimal resistance that would provide maximum power for the TENG was then determined. Since the TENG has a very small contact area between both its dielectric surfaces, a small power output was expected. The voltage and current output of the TENG were measured at various resistances as shown in Fig. 7. It shows that the logarithmic trendlines for current values and voltage values crossed and started to become stable at 40 MΩ, usually indicating that the optimal power output is at its highest when the TENG is experiencing an external load of 40 MΩ, the highest output current value for this resistance range was 0.0625 ηA on average at a 10 MΩ load while the highest value for output voltage was 2.6 V on average at 100 MΩ of load. The value of the optimal resistance for power output was confirmed when output power was plotted against load resistance as shown in Fig. 8. A low power output of 0.145 ηW was measured at a load of 40 MΩ, this low power however was the highest power output recorded for this sensor. This is not a concern considering that voltage reading was the most important variable for the wind speed sensing application.

Since the sensor was confirmed to be producing usable signals, calibrating it was the next step. Two plots were made, one between the voltage output of the TENG and the wind speed, and another between the rotational speed of the TENG and the wind speed, Figs. 9 and 10 respectively. The voltage output of the TENG increased linearly with wind speed due to an increased contact force between the two tribolayers as the wind speed increased. The TENG had a sensitivity of 0.3626 V / (ms^{-1}) at a resistance of 40 MΩ. The rotational speed of the TENG also increased linearly with wind speed at a rate of 0.3083 rps / (ms^{-1}). These results suggest that in real-life applications, both the voltage and rotational speed of the TENG can be monitored in order to figure out the wind speed, increasing the reliability of the sensor.

CONCLUSIONS

1. A rotating sensor based on sliding-mode TENG was made to measure wind speed using commercial and cheap PA and PTFE tribolayers.

2. The sensor has a low power output which makes it unusable as a power source in its current state, although future improvements can enhance its power output. The output voltage peaked at 2.6 V at a resistance of 100 MΩ and the current peaked at a value of 0.0625 ηA at a resistance of 10 MΩ. The high voltage value made it suitable for the wind speed sensor application.

3. The sensor had an optimal power output at a resistive load of 40 MΩ.

4. The sensor had a voltage sensitivity of 0.3626 V/(ms^{-1}) and a rotational speed sensitivity of 0.3083 RPS/(ms^{-1}), having two methods of figuring out the wind speed increases its reliability.

REFERENCES

1. Al-Kabbany A. M., and Ali W. Y., "Reducing the electrostatic charge of polyester by blending by polyamide strings", Journal of the Egyptian Society of Tribology, Vol. 16, No. 4, pp. 36–44, (2019).

2. Ali A. S., "Triboelectrification of Synthetic Strings", Journal of the Egyptian Society of Tribology, Vol. 16, No. 2, pp. 26–36, (2019).

3. Wang Z. L., Lin L., Chen J., Niu S., Zi Y., Wang Z. L., Lin L., Chen J., Niu S., and Zi Y., "Triboelectrification", Triboelectric Nanogenerators, pp. 1–19, (2016).

4. Schein L. B., Castle G. P., and Lacks D. J., "Triboelectrification", Wiley Encyclopedia of Electrical and Electronics Engineering, pp. 1–14, (1999).

5. Tian H., and Lee J. J., "Electrostatic discharge damage of MR heads", IEEE transactions on magnetics, Vol. 31, No. 6, pp. 2624–2626, (1995).

6. Ali A. S., Youssef M. M., Ali W. Y., and Rashed A., "Enhancing the Efficiency of Triboelectric Nanogenerator by Electrostatic Induction", Journal of the Egyptian Society of Tribology, Vol. 20, No. 1, pp. 41–50, (2023).

7. Zou H., Zhang Y., Guo L., Wang P., He X., Dai G., Zheng H., Chen C., Wang A.C., Xu C. and Wang Z.L., "Quantifying the triboelectric series," Nature communications, Vol. 10, No. 1, p. 1427, (2019).

8. Diaz A., and Felix-Navarro R., "A semi-quantitative tribo-electric series for polymeric materials: the influence of chemical structure and properties", Journal of Electrostatics, Vol. 62, No. 4, pp. 277–290, (2004).

9. Burgo T. A., Galembeck F., and Pollack G. H., "Where is water in the triboelectric series?", Journal of Electrostatics, Vol. 80, pp. 30–33, (2016).

10. Fan F.-R., Tian Z.-Q., and Lin Wang Z., "Flexible triboelectric generator", Nano Energy, Vol. 1, No. 2, pp. 328–334, (2012).

11. Han J., Feng Y., Chen P., Liang X., Pang H., Jiang T., and Wang Z. L., "Wind-driven soft-contact rotary triboelectric nanogenerator based on rabbit fur with high performance and durability for smart farming", Advanced Functional Materials, Vol. 32, No. 2, p. 2108580, (2022).

12. Yang Y., Zhu G., Zhang H., Chen J., Zhong X., Lin Z.-H., Su Y., Bai P., Wen X., and Wang Z. L., "Triboelectric nanogenerator for harvesting wind energy and as self-powered wind vector sensor system", ACS nano, Vol. 7, No. 10, pp. 9461–9468, (2013).

13. Zhang H., Yang Y., Su Y., Chen J., Adams K., Lee S., Hu C., and Wang Z. L., "Triboelectric nanogenerator for harvesting vibration energy in full space and as self-powered acceleration sensor", Advanced Functional Materials, Vol. 24, No. 10, pp. 1401–1407, (2014).
14. Cheng P., Guo H., Wen Z., Zhang C., Yin X., Li X., Liu D., Song W., Sun X., Wang J., and Wang Z. L., "Largely enhanced triboelectric nanogenerator for efficient harvesting of water wave energy by soft contacted structure", Nano Energy, Vol. 57, pp. 432–439, (2019).
15. Wang X., Niu S., Yin Y., Yi F., You Z., and Wang Z. L., "Triboelectric nanogenerator based on fully enclosed rolling spherical structure for harvesting low-frequency water wave energy", Advanced Energy Materials, Vol. 5, No. 24, p. 1501467, (2015).
16. Mousa H. M., Arafat A. G., Omran A.-N. M., and Abdel-Jaber G., "A hybrid triboelectric and piezoelectric nanogenerator with α-Al2O3 NPs/Doku and PVDF/SWCNTs nanofibers", Colloids and Surfaces A: Physicochemical and Engineering Aspects, Vol. 656, p. 130403, (2023).
17. Dhakar L., Pitchappa P., Tay F. E. H., and Lee C., "An intelligent skin based self-powered finger motion sensor integrated with triboelectric nanogenerator", Nano Energy, Vol. 19, pp. 532–540, (2016).
18. Zhou Q., Pan J., Deng S., Xia F., and Kim T., "Triboelectric nanogenerator-based sensor systems for chemical or biological detection", Advanced Materials, Vol. 33, No. 35, p. 2008276, (2021).
19. Qin K., Chen C., Pu X., Tang Q., He W., Liu Y., Zeng Q., Liu G., Guo H., and Hu C., "Magnetic array assisted triboelectric nanogenerator sensor for real-time gesture interaction", Nano-micro letters, Vol. 13, pp. 1–9, (2021).
20. Jin T., Sun Z., Li L., Zhang Q., Zhu M., Zhang Z., Yuan G., Chen T., Tian Y., Hou X., and Lee. C., "Triboelectric nanogenerator sensors for soft robotics aiming at digital twin applications", Nature communications, Vol. 11, No. 1, p. 5381, (2020).
21. Xia K., Du C., Zhu Z., Wang R., Zhang H., and Xu Z., "Sliding-mode triboelectric nanogenerator based on paper and as a self-powered velocity and force sensor", Applied Materials Today, Vol. 13, pp. 190–197, (2018).
22. Fan F.-R., Lin L., Zhu G., Wu W., Zhang R., and Wang Z. L., "Transparent triboelectric nanogenerators and self-powered pressure sensors based on micropatterned plastic films", Nano letters, Vol. 12, No. 6, pp. 3109–3114, (2012).
23. Zhu G., Pan C., Guo W., Chen C.-Y., Zhou Y., Yu R., and Wang Z. L., "Triboelectric-generator-driven pulse electrodeposition for micropatterning", Nano letters, Vol. 12, No. 9, pp. 4960–4965, (2012).
24. Kim D., Tcho I.-W., and Choi Y.-K., "Triboelectric nanogenerator based on rolling motion of beads for harvesting wind energy as active wind speed sensor", Nano Energy, Vol. 52, pp. 256–263, (2018).
25. Wang J., Ding W., Pan L., Wu C., Yu H., Yang L., Liao R., and Wang Z. L., "Self-powered wind sensor system for detecting wind speed and direction based on a triboelectric nanogenerator", ACS nano, Vol. 12, No. 4, pp. 3954–3963, (2018).